Environmental Science & Technology Letters

pubs.acs.org/journal/estlcu

Letter

Networks of Dissolved Organic Matter and Organo-Mineral Associations Stimulate Electron Transfer over Centimeter Distances

Yuge Bai,*[,∇] Tianran Sun,[∇] Muammar Mansor, Prachi Joshi, Yiling Zhuang, Stefan B. Haderlein, Stefan Fischer, Kurt O. Konhauser, Daniel S. Alessi, and Andreas Kappler*

Cite This: https://doi.org/10.1021/acs.estlett.3c00172

Read Online

ACCESS | Metrics & More | Article Recommendations | Supporting Information

ABSTRACT: Natural organic matter (NOM) dominated electron transfer has been widely studied in wetlands, freshwater sediments, and peatlands, in which a diffusion-electron hopping mechanism consisting of dissolved organic matter (DOM) and particulate organic matter (POM) was found to mediate electron transfer over centimeter (cm) distances. However, it remains unclear whether such long-distance electron transfer also occurs when NOM is associated with minerals, which form organo-mineral associations (OMAs) and thus are less mobile and accessible. In this study, we investigated the roles of DOM and OMAs in transferring electrons by performing a series of microbial Fe(III)-mineral reduction experiments over a 2 cm distance. We found that significant electron transfer only occurred when both DOM and OMAs were present. Generally, we observed a positive correlation between the relative proportion of DOM and OMAs and the extent of Fe(III) mineral reduction. However, varying the proportion of DOM showed a stronger effect on the Fe(III)-mineral reduction compared to OMAs, indicating that DOM played a more critical role in the electron transfer network. Our findings shed new light on how organic carbon facilitates iron transformation and the associated biogeochemical cycling of nutrients and contaminants in forest soil systems.

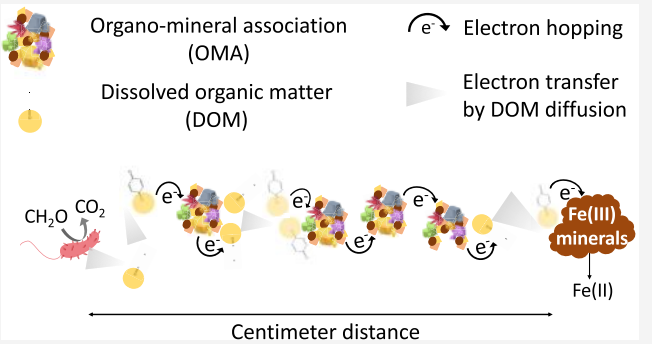

KEYWORDS: *dissolved organic matter (DOM), organo-mineral associations (OMAs), long-distance electron transfer, Fe(III) minerals*

INTRODUCTION

Extracellular electron transfer between microbes and terminal electron acceptors (e.g., SO_4^{2-}, NO_3^- or ferric iron (Fe(III)) minerals) under anoxic conditions has been widely studied in wetlands, freshwater sediments, and peat soils.[1−3] Redox-active natural organic matter (NOM)[4] has been considered one of the most important mediators of extracellular electron transfer in these systems.[5−7] NOM consists of dissolved organic matter (DOM), particulate organic matter (POM), and organic matter associated with minerals (i.e., organo-mineral associations, OMAs).[8−11] Although existing in lower concentrations, DOM can transfer electrons by diffusion with a coefficient of 10^{-6} cm^2 s^{-1} in the liquid phase, whereas POM and OMAs possess very low mobility.[12] However, previous studies have shown that POM can interact with DOM via electron hopping, i.e., electron self-exchange reactions among their redox-active centers.[13] The interaction between DOM and POM can promote the formation of a network that facilitates long-distance electron transfer at centimeter (cm) scales.[14,15]

DOM and OMAs have also been shown to exist in a dynamic equilibrium with continuous electron exchange,[16,17] which highly resembles the diffusion-electron hopping mechanism for electron transfer over cm distances with DOM and POM as mediators.[15,18] However, thus far, it is still unclear whether such long-distance electron transfer can occur within DOM and OMAs. The formation of OMAs includes coprecipitation, complexation, and adsorption, all of which increase their stability and protect the organic matter from decomposition and degradation.[19] However, studies have shown that OMAs are redox-active due to both the functional groups in the organic matter fraction and the redox-active centers of the Fe and manganese (Mn) mineral phases.[20−22] OMAs are ubiquitous and can contribute up to 90% to the NOM pool in some soil systems.[23] Given the wide existence of OMAs, a better understanding of their electron transfer properties and interactions with DOM is needed to improve our understanding of the electron flow as well as organic carbon transformation in ecosystems.

In this study, forest soil was used as an example to investigate the ability of DOM and OMAs in sustaining long-distance electron transfer processes. *Shewanella oneidensis* MR-

Received: March 7, 2023
Revised: May 17, 2023
Accepted: May 18, 2023

1, a well-known Fe(III) mineral-reducing bacterium, was used as the electron-donating bacterial strain.[24] Ferrihydrite (simplified: $Fe(OH)_3$), an environmentally common Fe(III) mineral, was used as the terminal electron acceptor. The DOM and OMAs samples were extracted from a forest soil, mixed at different ratios, and added as electron mediators in between the spatially separated *S. oneidensis* MR-1 and ferrihydrite over 2 cm distance in agar-solidified reactors as described earlier[25] and shown in Figure S1. Our objectives in this study were to (1) evaluate the possibility of electron transfer over cm distances with a network formed by DOM and OMAs and (2) determine the relative contribution of DOM and OMAs in mediating long-distance electron transfer.

MATERIALS AND METHODS

Soil Sampling and Separation of DOM and OMAs. Surface (0−10 cm) soil samples were collected from the Schönbuch forest in Germany (48°61′ N, 9°12′ E). The DOM and OMAs were obtained by washing the soil samples with Milli-Q water (resistivity 18.2 MΩ·cm), followed by size separation. Details on the sampling site and the separation procedure are shown in S1 of the Supporting Information (SI).

DOM and OMA Characterization. The elemental composition of OMAs was analyzed by inductively coupled plasma mass spectrometry (ICP-MS) after microwave-assisted acid digestion. Surface morphology and elemental distribution of OMAs were probed by scanning electron microscopy (SEM) combined with energy dispersive X-ray analysis (EDS). The redox properties of DOM and OMAs were characterized using a mediated electrochemical method.[26] Details of these analyses are provided in the SI (S2−S4).

Electron Transfer Experiment Setup and Sampling Procedure. All electron transfer experiments were carried out in agar-solidified reactors (Figure S1). Briefly, an agar ball containing 10 mmol L^{-1} ferrihydrite was positioned in the center of a Schott bottle. The ball was surrounded by 2% agar amended with DOM and OMAs as electron mediators. On top of the agar, 10^8 cells mL^{-1} *S. oneidensis* MR-1 were inoculated with 10 mM lactate as the electron donor. The electron transfer distance was 2 cm, and HEPES buffer (30 mM) was used to maintain the pH at approximately 7. We performed two sets of experiments. One set was with a fixed DOM concentration of 50 mg C L^{-1} but increasing OMA concentrations from 0 to 1600 mg C L^{-1}. The other set was with a fixed OMA concentration of 800 mg C L^{-1} but increasing DOM concentrations from 0 to 100 mg C L^{-1}. These concentrations are environmentally relevant according to previous studies,[10,27] and a more detailed discussion can be found in S8 of the SI. A series of reactors were set up so that they could be sacrificed over time during the course of the experiment. The headspace of all reactors was flushed with dinitrogen gas (N_2). For the cultivation of *S. oneidensis* MR-1, the synthesis of ferrihydrite, the experimental setup, and the sampling procedure, refer to the SI (S5−S7).

RESULTS AND DISCUSSION

Morphology and Elemental Composition of OMAs. The extracted OMAs had a particle size of ca. 400 μm as evidenced by the SEM images (Figures 1 and S2). Analyses using an elemental analyzer determined a total organic carbon content of 16.1 ± 1.5% (w/w) in bulk OMAs. Al and Fe were detected and quantified by ICP-MS at 27.2 and 6.4 mg g^{-1}, respectively (Figure S3). The overlapping distribution patterns of carbon (C), oxygen (O), and silica (Si) shown in the EDS mapping suggests a close association of these elements (Figure 1). Together, the data show the existence of OMAs. Previous studies revealed that the formation of primary OMAs involved the binding of functional groups of organic molecules (e.g., proteins, cellulose) with the surface of kaolin-group minerals such as kaolinite ($Al_2Si_2O_5(OH)_4$) or antigorite ((Mg,

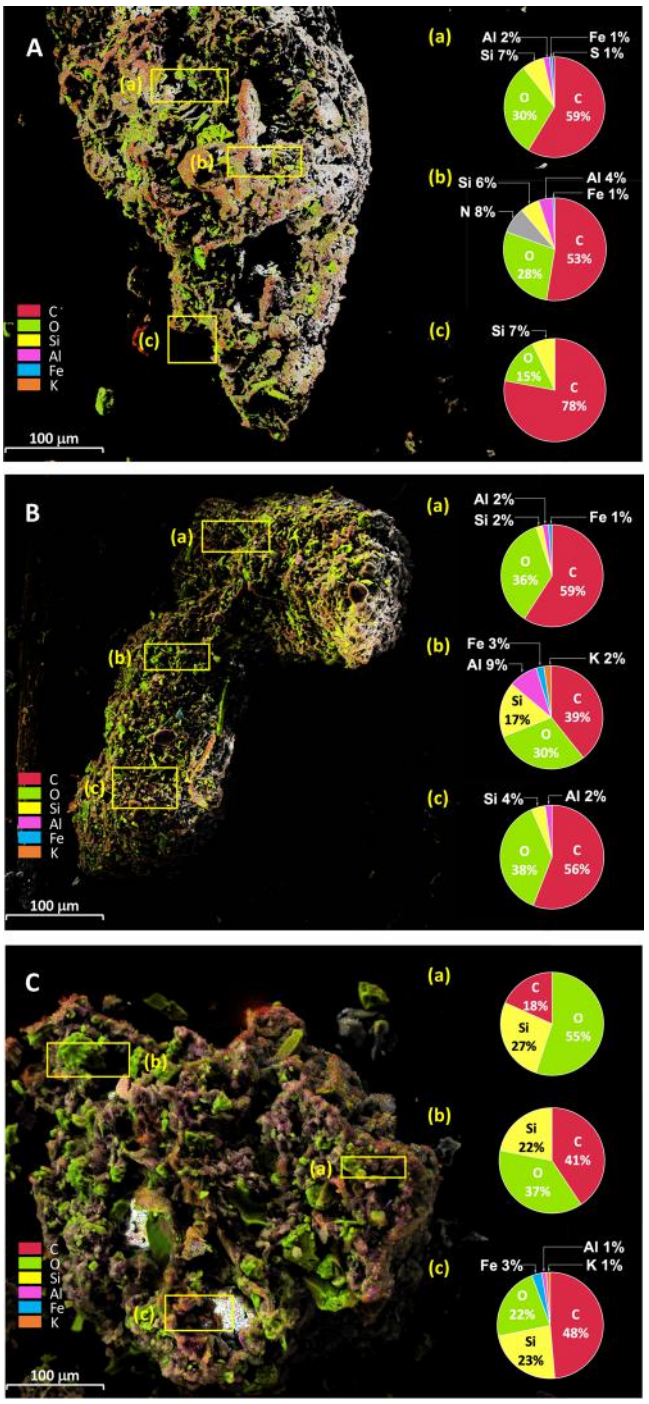

Figure 1. SEM micrographs coupled to EDS mapping of three OMA samples. The pie charts indicate the elemental composition of the three selected spots as shown on the SEM micrographs. Minor elements such as sulfur (S), nitrogen (N), and potassium (K) detected in random spots likely stem from plant and microorganism residues that are attached to the surface of OMAs.[35]

https://doi.org/10.1021/acs.estlett.3c00172
Environ. Sci. Technol. Lett. XXXX, XXX, XXX−XXX

$Fe^{2+})_3Si_2O_5(OH)_4$) via van der Waals forces and hydrogen bonds.[28−31] In contrast to the primary OMAs complexes, which usually possess a size of up to 20 μm,[32] the OMA particles found in our samples were about 400 μm, suggesting the occurrence of secondary aggregation as previously observed by Christensen.[33] Secondary OMAs consist of primary OMA complexes, macroaggregates, and coprecipitated organic matter moieties. Therefore, they are less dense and more reactive, and allow a faster flow of nutrients.[33−35]

Redox Activities of the Extracted DOM and OMAs. We used mediated electrochemical reduction and oxidation to characterize the electron accepting and donating capacity (EAC and EDC, respectively) of the extracted DOM and OMAs. As shown in Figure 2A, DOM has an EDC of 3963 ± 207 μmol e^- g^{-1} C and an EAC of 659 ± 41 μmol e^- g^{-1} C. Previous studies showed that EDC is primarily determined by the phenol content and EAC largely reflects the number of quinones.[36,37] Therefore, the much higher EDC than EAC in our DOM sample indicates high phenols and low quinones, potentially due to the high lignin content in the Schönbuch forest soil where the DOM was extracted from.[37] The same trend of EDC versus EAC was also found in some standard humic substances such as the Washkish Peat Humic Acid (WPHA), which was isolated from a sphagnum bog containing poorly degraded materials such as lignin.[37] Interestingly, although being isolated from the same soil, in contrast to DOM, the OMA samples showed a similar EDC (1164 ± 82 μmol e^- g^{-1} C) and EAC (1416 ± 200 μmol e^- g^{-1} C) (Figure 2A). We believe that the high EAC in the OMAs can be attributed to the presence of electron-accepting minerals such as Fe(III) in the OMAs. Moreover, compared to the electron exchange capacity (EEC: EAC + EDC) of DOM (4622 μmol e^- g^{-1} C), the EEC of the OMAs (2580 μmol e^- g^{-1} C) is much smaller, indicating a smaller density of electron-donating and accepting moieties on the surface of OMAs than that of DOM.

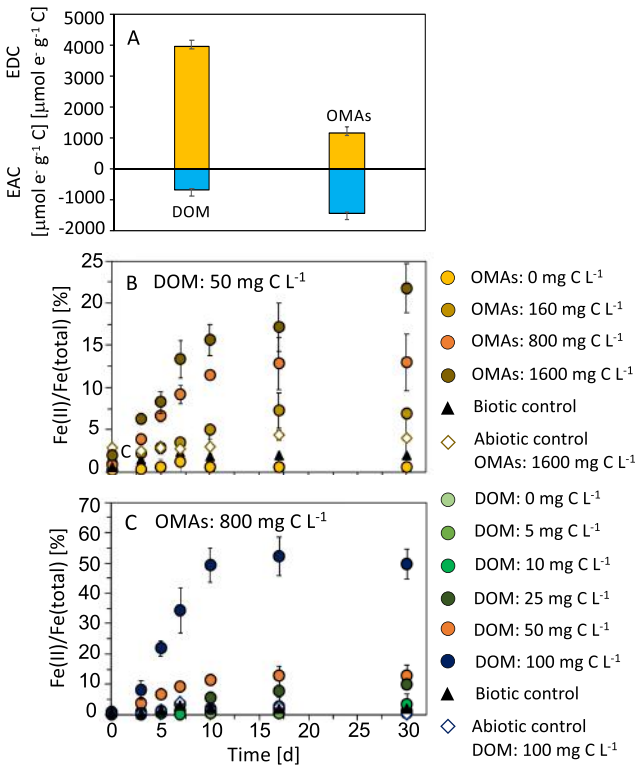

Figure 2. (A) Electron exchange capacity (EEC), the sum of electron-donating capacity (EDC) and electron-accepting capacity (EAC) of the DOM and OMAs extracted from the Schönbuch forest soil. All EDC and EAC values were normalized to the carbon content in DOM and OMAs. Error bars represent the standard deviation of at least four replicates. (B, C) Results from the microbial reduction of 10 mmol L^{-1} ferrihydrite by 10^8 cells mL^{-1} of *Shewanella oneidensis* MR-1 in the presence of 10 mmol L^{-1} lactate as electron donor, 50 mg C L^{-1} DOM with different concentrations of OMAs (B) or 800 mg C L^{-1} OMAs with varies concentrations of DOM (C) were used as electron shuttles. All experiments were conducted with the agar-solidified reactor as shown in Figure S1 with a 2 cm shuttling distance and incubated at 30 °C in the dark. At each sampling point, the ferrihydrite agar ball located at the bottle's center was taken out and dissolved in 1 M HCl for 1 h in an anoxic glovebox (100% N_2) for Fe extraction, and the Fe(II) and Fe(total) concentrations in the agar-ferrihydrite ball were quantified using the spectrophotometric ferrozine assay.[38] Data are means from triplicate bottles ± standard deviation, shown as the ratio of Fe(II) to Fe (total) in the ferrihydrite. The data set of DOM concentration as 50 mg C L^{-1} and OMA concentration as 800 mg C L^{-1} (orange circle) are from one single experiment and are identical in panels B and C.

Synergistic Effect of DOM and OMAs in Enabling Long-Distance Electron Transfer. Electron transfer over a 2 cm distance between *S. oneidensis* MR-1 and ferrihydrite was monitored over time. In the biotic controls (i.e., experiments without the addition of DOM or OMAs), no significant ferrihydrite reduction was detected, demonstrating that the solidified agar successfully prevented direct microbial ferrihydrite reduction. In contrast, up to 50% ferrihydrite reduction took place in experiments amended with DOM and OMAs, demonstrating their abilities in mediating long-distance electron transfer. In the treatments with a fixed DOM concentration (50 mg C L^{-1}), no significant ferrihydrite reduction was observed without the addition of OMAs. Increasing the OMA concentrations from 160 to 800 to 1600 mg L^{-1} increased the extent of ferrihydrite reduction from 6.83 ± 0.57% to 12.98 ± 3.40% to 21.78 ± 2.90% (Figure 2B). A similar result was also found in the reversed experiments where we fixed the OMA concentration at 800 mg C L^{-1} (Figure 2C). In the absence of DOM, no significant ferrihydrite reduction was observed. By increasing the amount of DOM from 25 to 50 to 100 mg L^{-1}, however, the ferrihydrite reduction increased from 9.99 ± 0.73% to 12.98 ± 1.13% to 49.13 ± 4.87%, respectively.

Notably, significant ferrihydrite reduction occurred only when DOM and OMAs were present together. These results revealed, for the first time, that electron transfer at cm scales can occur with DOM and OMAs as electron mediators. Moreover, a synergistic effect occurred between DOM and OMAs, probably by the formation of a redox-cycling network that allowed a higher number of transferred electrons per time in comparison with either DOM or OMAs alone. Such a synergistic effect is in line with a diffusion-electron hopping mechanism[18] through which the diffusion of DOM could be largely shortened via electron hopping of OMAs, thus enhancing the overall electron transfer process.[15]

Electron Transfer Kinetics as a Function of the Ratio of DOM and OMAs. Based on the data shown in Figure 2B, C, we evaluated how the DOM:OMAs ratios affected the extent (Figure 3A) and rate (Figure S4) of ferrihydrite reduction. In general, the correlation between both the extent and rate of ferrihydrite reduction and DOM:OMAs ratios were

https://doi.org/10.1021/acs.estlett.3c00172
Environ. Sci. Technol. Lett. XXXX, XXX, XXX−XXX

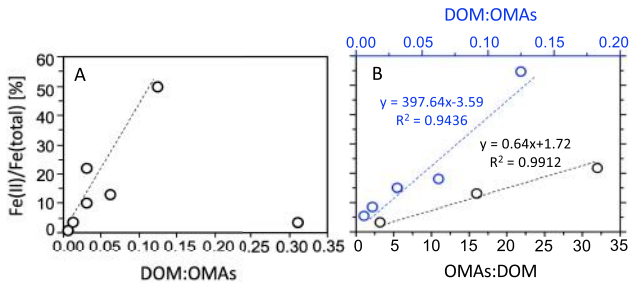

Figure 3. Correlation between the extent of ferrihydrite reduction and the DOM:OMAs ratios (A) and the correlation between the extent of ferrihydrite reduction and both the DOM:OMAs and OMAs:DOM ratios (B). Whereas the DOM:OMAs ratios in (A) were obtained from all the experiments as shown in Figure 2B, C, the DOM:OMAs ratios in (B) were collected from the experimental setups with fixed OMA concentration and variable DOM concentrations (Figure 2C). The OMAs:DOM ratios in (B) were obtained from the experiments with fixed DOM concentration but multiple OMA concentrations (Figure 2B). It should be noted that the same experiment with a DOM concentration of 50 mg C L^{-1} and OMA concentration of 800 mg C L^{-1} was plotted twice in (B), one point with DOM:OMAs of 0.06 and another point with OMAs:DOM of 16. This also explains why there is one more data point in (B) than in (A). The dashed line in (A) shows the linear fitting of 6 data points only, excluding the data point with a DOM:OMAs ratio of 0.31.

positive and showed high similarity. Yet, it should be noted that, even with the same ratio of DOM:OMAs, the absolute amount of DOM and OMAs also impacted the electron transfer rate. For example, although the treatment with a DOM concentration of 50 mg C L^{-1} and an OMA concentration of 1600 mg C L^{-1} and the treatment with a DOM concentration of 25 mg C L^{-1} and an OMA concentration of 800 mg C L^{-1} both resulted in a DOM:OMAs ratio of 0.03, the treatment with higher DOM and OMA content resulted in faster electron transfer kinetics (21.78 ± 2.90% ferrihydrite reduction) compared to the treatment with lower DOM and OMA content (9.99 ± 0.73% ferrihydrite reduction). The same phenomenon can also be found in the experiment having a DOM concentration of 50 mg C L^{-1} and an OMA concentration of 160 mg C L^{-1}. Although it resulted in a high DOM:OMAs ratio of 0.31, the generally low absolute amount of DOM and OMAs led to a markedly lower extent and rate of ferrihydrite reduction as compared to the other experiments (Figures 3A and S4). These results indicate that both the DOM:OMAs ratio and their absolute content should be considered for a comprehensive assessment of the electron transfer processes of DOM and OMAs.

Furthermore, we also evaluated correlations between the extent of ferrihydrite reduction and both the DOM:OMAs ratios and the OMAs:DOM ratios (Figure 3B). Whereas the OMAs:DOM ratios were calculated from the experiments with fixed DOM concentration and variable OMA concentrations (Figure 2B), the DOM:OMAs ratios were obtained from the experiments with fixed OMA concentration but varying DOM concentrations (Figure 2C). Although positive correlations were found between the extent of ferrihydrite reduction and both the DOM:OMAs and OMAs:DOM ratios, DOM:OMAs ratios were more decisive in accelerating ferrihydrite reduction, as evidenced by the higher slope of DOM:OMAs (397.64) than that of OMAs:DOM (0.64) in Figure 3B. These findings suggest that DOM played a more important role in the rate of redox cycling of the DOM and OMA network and thus dominated the overall electron transfer kinetics, which potentially results from its high EEC as shown in Figure 2A.

Implications. Previous studies investigated the electron transfer processes of DOM[39−41] and POM[3,42] as well as the combination of both.[14] However, OMA has long been overlooked despite its wide distribution in the environment.[43,44] The lack of studies regarding the electron transfer by OMAs might be due to the well-accepted concept that the organic matter in OMAs is protected from microbial and chemical decomposition.[10,30] Our study, however, shows that OMAs are redox active and can interact with DOM to constitute a network that promotes electron transfer over cm distances. Such long-distance electron transfer can impact other biogeochemical processes such as microbial Fe(III)-mineral reduction, which further affects the fate of contaminants such as arsenic (As), chromium (Cr), and uranium (U).[45−47] Fe(II) produced by Fe(III) reduction can be coupled to the degradation of organic contaminants including polyhalogenated compounds, nitroaromatics, and azo dyes.[45] Additionally, Fe(III)-mineral reduction can compete for electron transfer to methanogens and nitrate- and sulfate-reducing bacteria, thereby inhibiting greenhouse gas emissions.[48] With the increasing frequency of redox fluctuations due to alternating extreme drought and precipitation events,[49] we call for future studies to take such long-distance electron transfer into consideration when studying biogeochemical elemental cycling and the carbon budget estimates in the environment.

■ ASSOCIATED CONTENT

Supporting Information

The Supporting Information is available free of charge at https://pubs.acs.org/doi/10.1021/acs.estlett.3c00172.

Detailed experimental procedures including the extraction of DOM and OMAs from soil (S1), the total carbon and ICP-MS characterization of the extracted OMAs (S2), the SEM imaging of the extracted OMAs (S3), electrochemical analysis of DOM and OMAs (S4), cultivation of *S. oneidensis* MR-1 (S5), synthesis of ferrihydrite (S6), the ferrihydrite reduction experiment setup and samples procedure (S7), and the environmental relevance of the DOM and OMA concentrations in the experiment (S8); the agar-solidified experimental setup (Figure S1), the SEM image of selected OMA particles (Figure S2), the elemental composition of OMAs characterized by ICP-MS (Figure S3), and the correlation between the DOM:DOAs ratios and the rate of ferrihydrite reduction (Figure S4) (PDF)

■ AUTHOR INFORMATION

Corresponding Authors

Yuge Bai − *Geomicrobiology, Department of Geosciences, University of Tübingen, 72076 Tübingen, Germany; Department of Earth and Atmospheric Sciences, Faculty of Science, University of Alberta, Edmonton, Alberta T6G 2E3, Canada;* orcid.org/0009-0007-7331-5395; Email: yuge3@ualberta.ca

Andreas Kappler − *Geomicrobiology, Department of Geosciences, University of Tübingen, 72076 Tübingen, Germany; Cluster of Excellence: EXC 2124: Controlling Microbes to Fight Infection, Tübingen 72076, Germany;*

https://doi.org/10.1021/acs.estlett.3c00172
Environ. Sci. Technol. Lett. XXXX, XXX, XXX−XXX

orcid.org/0000-0002-3558-9500; Phone: +49-7071-2974992; Email: andreas.kappler@uni-tuebingen.de

Authors

Tianran Sun − *State Key Lab of Urban and Regional Ecology, Research Center for Eco-Environmental Sciences, Chinese Academy of Sciences, 10085 Beijing, China;* orcid.org/0000-0001-8679-1285

Muammar Mansor − *Geomicrobiology, Department of Geosciences, University of Tübingen, 72076 Tübingen, Germany;* orcid.org/0000-0001-7830-650X

Prachi Joshi − *Geomicrobiology, Department of Geosciences, University of Tübingen, 72076 Tübingen, Germany*

Yiling Zhuang − *Environmental Mineralogy and Chemistry, Department of Geosciences, University of Tübingen, 72076 Tübingen, Germany*

Stefan B. Haderlein − *Environmental Mineralogy and Chemistry, Department of Geosciences, University of Tübingen, 72076 Tübingen, Germany*

Stefan Fischer − *Tübingen Structural Microscopy Core Facility (TSM), University of Tübingen, 72076 Tübingen, Germany*

Kurt O. Konhauser − *Department of Earth and Atmospheric Sciences, Faculty of Science, University of Alberta, Edmonton, Alberta T6G 2E3, Canada*

Daniel S. Alessi − *Department of Earth and Atmospheric Sciences, Faculty of Science, University of Alberta, Edmonton, Alberta T6G 2E3, Canada;* orcid.org/0000-0002-8360-8251

Complete contact information is available at: https://pubs.acs.org/10.1021/acs.estlett.3c00172

Author Contributions

[▽]Y.B. and T.S. contributed equally to this work.

Notes

The authors declare no competing financial interest.

■ ACKNOWLEDGMENTS

We would like to thank Prof. Dr. Thomas Scholten, Dr. Monique Patzner, and Corinna Gall for their help with the soil sampling. Many appreciations go to Bernice Nisch and Sören Drabesch for analyzing the TOC and performing the ICP-MS of our soil samples, respectively. Many thanks to Marie Hoff for her assistance in the lab. We also thank Ellen Röhm for the development of the agar-solidified experimental setup and the preliminary tests, and we thank Lars Grimm, Franziska Schädler, and Lea Sauter for their technical support in the lab. A.K. acknowledges infrastructural support by the Deutsche Forschungsgemeinschaft (DFG, German Research Foundation) under Germany's Excellence Strategy, cluster of Excellence EXC2124, project ID 390838134. The authors gratefully acknowledge the Tübingen Structural Microscopy Core Facility (Funded by the Federal Ministry of Education and Research (BMBF) and the Baden-Württemberg Ministry of Science as part of the Excellence Strategy of the German Federal and State Governments) for their support and assistance in this work and thank the DFG (INST 37/1027-1 FUGG) for the financial support provided for the acquisition of the cryogenic focused ion beam scanning electron microscope used in this study at Tübingen University.

■ REFERENCES

(1) Walpen, N.; Getzinger, G. J.; Schroth, M. H.; Sander, M. Electron-donating phenolic and electron-accepting quinone moieties in peat dissolved organic matter: Quantities and redox trasnformations in the context of peat biogeochemistry. *Environ. Sci. Technol.* **2018**, *52* (9), 5236−5245.

(2) Mladenov, N.; Zheng, Y.; Miller, M. P.; Nemergut, D. R.; Legg, T.; Simone, B.; Hageman, C.; Rahman, M. M.; Ahmed, K. M.; McKnight, D. M. Dissolved organic matter sources and consequences for iron and arsenic mobilization in Bangladesh aquifers. *Environ. Sci. Technol.* **2010**, *44* (1), 123−128.

(3) Roden, E.; Kappler, A.; Bauer, I.; Jiang, J.; Paul, A.; Stoesser, R.; Konishi, H.; Xu, H. Extracellular electron trasnfer through microbial reduction of solid-phase humic substances. *Nat. Geosci.* **2010**, *3*, 417−421.

(4) Stevenson, F. J. *Humus chemistry: genesis, composition, reaction*; Wiley: New York, U.S.A., 1994.

(5) Nurmi, J. T.; Tratnyek, P. G. Electronchemical properties of natural organic matter (NOM), fractions of NOM, and model biogeochemical electron shuttles. *Environ. Sci. Technol.* **2002**, *36* (4), 617−624.

(6) Kappler, A.; Benz, M.; Schink, B.; Brune, A. Electron shuttling via humic acids in microbial iron (III) reduction in a freshwater sediment. *FEMS Microbiol. Ecol.* **2004**, *47* (1), 85−92.

(7) Sposito, G. Electron Shuttling by Natural Organic Matter: Twenty Years After. In *Aquatic Redox Chemistry*; Tratnyek, P. G., Grundl, T. J., Haderlein, S. B., Eds.; American Chemical Society, 2011; pp 113−127; DOI: 10.1021/bk-2011-1071.ch006.

(8) Lavallee, J. M.; Soong, J. L.; Cotrufo, M. F. Conceptualizing soil organic matter into particulate and mineral-associated forms to address global change in the 21st century. *Glob. Change Biol.* **2020**, *26*, 261−273.

(9) Nanthi, S.; et al. Dissolved organic matter: Biogeochemistry, dynamics, and environmental soils. In *Advances in Agronomy*; Sparks, D. L., Ed.; Academic Press, 2011; pp 1−75; DOI: 10.1016/B978-0-12-385531-2.00001-3.

(10) Kögel-Knabner, I.; Guggenberger, G.; Kleber, M.; Kandeler, E.; Kalbitz, K.; Scheu, S.; Eusterhues, K.; Leinweber, P. Organo-mineral association in temperate soils: Integrating biology, mineralogy, and oragnic matter chemistry. *J. Plant Nutr. Soil Sci.* **2008**, *171*, 61−82.

(11) Kleber, M.; Bourg, I. C.; Coward, E. K.; Hansel, C. M.; Myneni, S. C. B.; Nunan, N. Dynamic interactions at the mineral-organic matter interface. *Nat. Rev. Earth Environ.* **2021**, *2*, 402−421.

(12) Huskinson, B.; Marshak, M. P.; Suh, C.; Er, S.; Gerhardt, M. R.; Galvin, C. J.; Chen, X. D.; Aspuru-Guzik, A.; Gordon, R. G.; Aziz, M. J. A metal-free organic-inorganic aqueous flow battery. *Nature* **2014**, *505* (7482), 195−198.

(13) Blauch, D. N.; Saveant, J. M. Dynamics of electron hopping in assemblies of redox centers. Percolation and diffusion. *J. Am. Chem. Soc.* **1992**, *114* (9), 3323−3332.

(14) Gao, C.; Sander, M.; Agethen, S.; Knorr, K. Electron accepting capacity of dissolved and particulate organic matter control CO_2 and CH_4 formation in peat soils. *Geochim. Cosmochim. Acta* **2019**, *245*, 266−277.

(15) Bai, Y.; Sun, T.; Angnent, L. T.; Haderlein, S. B.; Kappler, A. Electron hopping enables rapid electron trasnfer between quinone-/hydroquinone-containing organic molecules in microbial iron(III) mineral reduction. *Environ. Sci. Technol.* **2020**, *54* (17), 10646−10653.

(16) Sanderman, J.; Baldock, J. A.; Amundson, R. Dissolved organic carbon chemistry and dynamics in contrasting forest and grassland soils. *Biogeochemistry* **2008**, *89*, 181−198.

(17) Torn, M. S.; Kleber, M.; Zavaleta, E.; Zhu, B.; Field, C.; Trumbore, S. A dual isotope approach to isolate carbon pools of different turnover times. *Biogeosciences* **2013**, *10* (12), 8067−8081.

(18) Sato, K.; Ichinoi, R.; Mizukami, R.; Serikawa, T.; Sasaki, Y.; Lutkenhaus, J.; Nishide, H.; Oyaizu, K. Diffusion-cooperative model for charge transport by redox-active nonconjugated polymers. *J. Am. Chem. Soc.* **2018**, *140* (3), 1049−1056.

(19) Witzgall, K.; Vidal, A.; Schubert, D. I.; Höschen, C.; Schweizer, S. A.; Buegger, F.; Pouteau, V.; Chenu, C.; Mueller, C. W. Particulate organic matter as a functional soil component for persistent soil organic carbon. *Nat. Commun.* **2021**, *12*, 4115.
(20) Lovley, D. R.; Holmes, D. E.; Nevin, K. P. Dissimilatory Fe(III) and Mn (IV) reduction. *Adv. Microb. Physiol.* **2004**, *49*, 219−286.
(21) Kappler, A.; Straub, K. L. Geomicrobiological cycling of iron. *Mol. Geomicrobiol.* **2005**, *59*, 85−108.
(22) Shimizu, M.; Zhou, J. H.; Schroder, C.; Obst, M.; Kappler, A.; Borch, T. Dissimilatory reduction and transformation of ferrihydrite-humic acid coprecipitates. *Environ. Sci. Technol.* **2013**, *47*, 13375−13384.
(23) Gabriel, C. E.; Kellman, L.; Prest, D. Examining mineral-associated soil organic matter pools through depth in harvested forest soil profiles. *PLoS One* **2018**, *13* (11), No. e0206847.
(24) Glasser, N. R.; Saunders, S. H.; Newman, D. K. The colorful world of extracellular electron shuttles. *Annu. Rev. Microbiol.* **2017**, *71*, 731−751.
(25) Bai, Y.; Mellage, A.; Cirpka, A. O.; Sun, T.; Angenent, L. T.; Haderlein, S. B.; Kappler, A. AQDS and redox-active NOM enables microbial Fe(III)-mineral reduction at cm-scales. *Environ. Sci. Technol.* **2020**, *54* (7), 4131−4139.
(26) Aeschbacher, M.; Sander, M.; Schwarzenbach, R. P. Novel electrochemical approach to assess the redox properties of humic substances. *Environ. Sci. Technol.* **2010**, *44*, 87−93.
(27) Michalzik, B.; Kalbitz, K.; Park, J. H.; Solinger, S.; Matzner, E. Fluxes and concentrations of dissolved organic carbon and nitrogen − a synthesis for temperate forest. *Biogeochemistry* **2001**, *52*, 173−205.
(28) Quiquampoix, H.; Abadie, J.; Baron, M. H.; Leprince, F.; Matumoto, P. T.; Ratcliffe, R. G.; Staunton, S. Mechanisms and consequences of protein adsorption on soil mineral surfaces. In *Proteins at Interfaces II Fundmentals and Applications*; Horbett, T. A., Brash, J. L., Eds.; American Chemical Society: Washington DC, 1995; pp 321−333; DOI: 10.1021/bk-1995-0602.ch023.
(29) Mikutta, R.; Kleber, M.; Torn, M. S.; Jahn, R. Stabilization of soil organic matter: As- sociation with minerals or chemical recalcitrance? *Biogeochemistry* **2006**, *77*, 25−56.
(30) Cuba-Chiem, L. T.; Huynh, L.; Ralston, J.; Beattie, D. A. In situ particle film ATR-FTIR spectroscopy of carboxymethyl cellulose adsorption on talc: binding mechanism, pH effects, and adsorption kinetics. *Langmuir* **2008**, *24*, 8036−8044.
(31) Kleber, M. et al. Mineral−organic associations: Formation, properties, and relevance in soil environments. In *Advances in Agronomy*; Sparks, D. L., Ed.; Academic Press, 2015; pp 1−140; DOI: 10.1016/bs.agron.2014.10.005.
(32) Beare, M. H.; Bruce, R. R. A comparison of methods for measuring water-stable aggregates: implications for determining environmental effects on soil structure. *Geoderma* **1993**, *56*, 87−104.
(33) Christensen, B. T. Physical fractionation of soil and structural and functional complexity in organic matter turnover. *Eur. J. Soil Sci.* **2001**, *52*, 345−353.
(34) Oades, J. M. The role of biology in the formation, stabilization and degradation of soil structure. *Geoderma* **1993**, *56*, 377−400.
(35) Possinger, A. R.; Zachman, M. J.; Enders, A.; Levin, B. D. A.; Müller, D. A.; Kourkoutis, L. F.; Lehmann, J. Organo−organic and organo−mineral interfaces in soil at the nanometer scale. *Nat. Commun.* **2020**, *11*, 6103.
(36) Argyropoulos, D. S.; Zhang, L. M. Semiquantitative determination of quinonoid structures in isolated lignins by P-31 nuclear magnetic resonance. *J. Agric. Food Chem.* **1998**, *46*, 4628−4634.
(37) Aeschbacher, M.; Graf, C.; Schwarzenbach, R. P.; Sander, M. Antioxidant properties of humic substances. *Environ. Sci. Technol.* **2012**, *46*, 4916−4925.
(38) Stookey, L. L. Ferrozine − A new spectrophotometric reagent for iron. *Anal. Chem.* **1970**, *42* (7), 779−781.
(39) Bauer, M.; Heitmann, T.; Macalady, D. L.; Blodau, C. Electron transfer capacities and reaction kinetics of peat dissolved organic matter. *Environ. Sci. Technol.* **2007**, *41*, 139−145.
(40) Jiang, J.; Kappler, A. Kinetics of microbial and chemical reduction of humic substances: Implications for electron shuttling. *Environ. Sci. Technol.* **2008**, *42* (10), 3563−3569.
(41) Yuan, T.; Yuan, Y.; Zhou, S.; Li, F.; Liu, Z.; Zhuang, L. A rapid and simple electrochemical method for evaluating the elctron transfer capacities of dissolved organic matter. *J. Soils Sediments* **2011**, *11*, 467−473.
(42) Joshi, P.; Schroth, M. H.; Sander, M. Redox properties of pear particulate organic matter: quantification of electron accepting capacities and assessment of electron transfer reversibility. *J. Geophys.Res. Biogeosci.* **2021**, *126*, 6329.
(43) Torn, M. S.; Trumbore, S. E.; Chadwick, O. A.; Vitousek, P. M.; Hendricks, D. M. Mineral control of soil organic carbon storage and turnover. *Nature* **1997**, *389*, 170−173.
(44) Possinger, A. R.; Zachman, M. J.; Ender, A.; Levin, B. D. A.; Müller, D. A.; Kourkoutis, L. F.; Lehmann, J. Organo-organic and organo-mineral interfaces in soil at the nanometer scale. *Nat. Commun.* **2020**, *11*, 6103.
(45) Borch, T.; Kretzschmar, R.; Kappler, A.; Van Cappellen, P.; Ginder-Vogel, M.; Voegelin, A.; Campbell, K. Biogeochemical redox processes and their impact on contaminant dynamics. *Environ. Sci. Technol.* **2010**, *44* (1), 15−23.
(46) Roberts, H. E.; Morris, K.; Law, G. T. W.; Mosselmans, J. F. W.; Bots, P.; Kvashnina, K.; Shaw, S. Uranium(V) incorporation mechanisms and stability in Fe(II)/Fe(III) (oxyhydr)oxides. *Environ. Sci. Technol. Lett.* **2017**, *4* (10), 421−426.
(47) Sundman, A.; Vitzthum, A. L.; Adaktylos-Surber, K.; Figueroa, A. I.; van der Laan, G.; Daus, B.; Kappler, A.; Byrne, J. M. Effect of Fe-metabolizing bacteria and humic substances on magnetite nano-particle reactivity towards arsenic and chromium. *J. Hazard. Mater.* **2020**, *384*, 121450.
(48) Valenzuela, E. I.; Padilla-Loma, C.; Gomez-Hernandez, N.; Lopez-Lozano, N. E.; Casas-Flores, S. Humic substances mediate anaerobic methane oxidation linked to nitrous oxide reduction in wetland sediments. *Front. Microbiol.* **2020**, *11*, 587.
(49) Tabari, H. Climate change impact on flood and extreme precipitation increases with water availability. *Sci. Rep.* **2020**, *10*, 13768.

https://doi.org/10.1021/acs.estlett.3c00172
Environ. Sci. Technol. Lett. XXXX, XXX, XXX−XXX